A&A 470, 353–357 (2007)
DOI: 10.1051/0004-6361:20077246


Astronomy & Astrophysics

# Torsional oscillations of longitudinally inhomogeneous coronal loops

T. V. Zaqarashvili[1] and K. Murawski[2]

[1] Georgian National Astrophysical Observatory (Abastumani Astrophysical Observatory), Kazbegi Ave. 2a, Tbilisi 0160, Georgia
e-mail: temury@genao.org
[2] Group of Astrophysics and Gravity Theory, Institute of Physics, UMCS, ul. Radziszewskiego 10, 20-031 Lublin, Poland

Received 6 February 2007 / Accepted 26 March 2007

**ABSTRACT**

*Aims.* We explore the effect of an inhomogeneous mass density field on frequencies and wave profiles of torsional Alfvén oscillations in solar coronal loops.
*Methods.* Dispersion relations for torsional oscillations are derived analytically in limits of weak and strong inhomogeneities. These analytical results are verified by numerical solutions, which are valid for a wide range of inhomogeneity strength.
*Results.* It is shown that the inhomogeneous mass density field leads to the reduction of a wave frequency of torsional oscillations, in comparison to that estimated from mass density at the loop apex. This frequency reduction results from the decrease of an average Alfvén speed as far as the inhomogeneous loop is denser at its footpoints. The derived dispersion relations and wave profiles are important for potential observations of torsional oscillations which result in periodic variations of spectral line widths.
*Conclusions.* Torsional oscillations offer an additional powerful tool for the development of coronal seismology.

**Key words.** magnetohydrodynamics (MHD) – Sun: corona – Sun: oscillations

## 1. Introduction

Recent space-based observations revealed the presence of various kinds of magnetohydrodynamic (MHD) waves and oscillations in the solar corona. These observations as well as modeling of MHD waves are important as these waves contribute to the coronal heating problem (Roberts 2000) and they may provide a unique tool for coronal seismology (Edwin & Roberts 1983; Nakariakov & Ofman 2001). Fast kink (Aschwanden et al. 1999; Nakariakov et al. 1999; Wang & Solanki 2004) and sausage (Nakariakov 2003; Pascoe et al. 2007) as well as slow (de Moortel et al. 2002; Wang et al. 2003) magnetosonic oscillations were observed to be associated either with or without a solar flare. Analytical studies of these oscillations in coronal loops were carried out over the last few decades, amongst others, by Edwin & Roberts (1982, 1983), Poedts & Boynton (1996), Nakariakov (2003), Van Doorsselaere et al. (2004a,b), Ofman (2005), Verwichte et al. (2006) and Diáz et al. (2006).

Coronal loops act as natural wave guides for magnetosonic and torsional Alfvén waves. The latter are purely azimuthal oscillations in cylindrical geometry. In the linear regime, Alfvén oscillations do not lead to mass density perturbations. As a result, contrary to magnetosonic waves, torsional Alfvén waves can be observed only spectroscopically. While propagating from the base of the solar corona along open magnetic field lines, these waves may lead to an increase of a spectral line width with height (Hassler et al. 1990; Banerjee et al. 1998; Doyle et al. 1998). In closed magnetic field structures, such as coronal loops, these waves can be observed indirectly as periodic variations of non-thermal broadening of spectral lines (Zaqarashvili 2003).

Alongside magnetosonic waves, torsional oscillations can be used to infer, in the framework of coronal seismology, plasma properties inside oscillating loops. These oscillations are an ideal tool for coronal seismology as their phase speed depends on plasma quantities within the loop alone, while wave speeds of magnetosonic oscillations are influenced by plasma conditions in the ambient medium. Having a known mass density within a loop, coronal seismology, that is based on torsional oscillations, enables us to estimate a magnetic field strength. Azimuthal Alfvén oscillations are potentially important in the context of rapid attenuation of coronal loop kink oscillations (Aschwanden et al. 1999; Nakariakov et al. 1999). One of a few suggested mechanisms of the attenuation is a resonant absorption of fast magnetosonic kink waves by azimuthal quasi-Alfvén waves (Ruderman & Roberts 2002). This process may lead to a formation of azimuthal oscillations in the outer part of a loop. As a result, spotting azimuthal torsional oscillations after the kink mode was attenuated would serve as evidence of this attenuation mechanism.

A theoretical study of Alfvén oscillations in a coronal loop was carried out recently by Gruszecki et al. (2007) who considered impulsively generated oscillations in two-dimensional straight and curved magnetic field topologies. They found that lateral leakage of Alfvén waves into the ambient corona is negligibly small. However, mass density profiles were assumed to be homogeneous within the loop, while the real conditions there are much more complex.

Despite the significant achievements in a development of realistic models, there is still much more effort required to develop our knowledge of wave phenomena in coronal loops. A goal of this paper is to study the influence of inhomogeneous mass density fields on the spectrum of torsional oscillations. The paper is organized as follows. Analytical solutions for torsional oscillations in a longitudinally inhomogeneous coronal loop are presented in Sect. 2. The numerical results are shown in Sect. 3. Guidelines for potential observations of these oscillations are

presented in Sect. 4. This paper concludes with a discussion and a short summary of the main results in Sect. 5.

## 2. Analytical model of torsional oscillations

We consider a coronal loop of inhomogeneous mass density $\varrho_0(z)$ and length $2L$, that is embedded in a uniform magnetic field $\boldsymbol{B} = B_0\hat{\boldsymbol{z}}$. Small amplitude torsional Alfvén waves in a cylindrical coordinate system $(r, \phi, z)$, in which plasma profiles depend on a longitudinal coordinate $z$ only, can be described by the following linear equations:

$$\frac{\partial u_\phi}{\partial t} = \frac{B_0}{4\pi\varrho_0(z)}\frac{\partial b_\phi}{\partial z}, \quad (1)$$

$$\frac{\partial b_\phi}{\partial t} = B_0\frac{\partial u_\phi}{\partial z}, \quad (2)$$

where $u_\phi$ and $b_\phi$ are the velocity and magnetic field components of Alfvén waves.

These equations can be easily cast into a single wave equation

$$\frac{\partial^2 u_\phi}{\partial z^2} - \frac{1}{V_{\rm A}^2(z)}\frac{\partial^2 u_\phi}{\partial t^2} = 0\,, \quad (3)$$

where $V_{\rm A}(z) = B_0/\sqrt{4\pi\varrho_0(z)}$ is the Alfvén speed. Assuming that $u_\phi \sim \exp(i\omega t)$, where $\omega$ is a wave frequency, we get the equation

$$\frac{\partial^2 u_\phi}{\partial z^2} + \frac{\omega^2}{V_{\rm A}^2}u_\phi = 0. \quad (4)$$

For a trapped solution, $u_\phi$ must satisfy line-tying boundary conditions which are implemented by setting

$$u_\phi(z = \pm L) = 0. \quad (5)$$

Equation (4) with condition (5) constitutes the well-known Sturm-Liouville problem whose solution depends on the profile of $V_{\rm A}(z)$. We model the coronal loop by a rarefied plasma at the loop apex (at $z = 0$) and by a compressed plasma at the loop footpoints ($z = \pm L$). Specifically, we adopt

$$\varrho_0(z) = \varrho_{00}\left(1 + \alpha^2\frac{z^2}{L^2}\right), \quad (6)$$

where $\varrho_{00}$ is the mass density at the loop apex and $\alpha^2$ is a parameter which defines the strength of the inhomogeneity. For $\alpha^2 = 0$ the above mass density profile corresponds to a homogeneous loop, while for a larger value of $\alpha^2$ the medium is more inhomogeneous. Figure 1 illustrates $\varrho_0(z)$ for $\alpha^2 = 50$. The mass density is described by Eq. (6) with $\varrho_{00} = 10^{-12}$ kg m$^{-3}$ and $L = 25$ Mm. Note that plasma is compressed at $z = \pm L$. Substituting Eq. (6) into Eq. (4), we obtain

$$\frac{\partial^2 u_\phi}{\partial z^2} + \frac{\omega^2}{V_{\rm A0}^2}\left(1 + \alpha^2\frac{z^2}{L^2}\right)u_\phi = 0\,, \quad (7)$$

where $V_{\rm A0} = B_0/\sqrt{4\pi\varrho_{00}}$. With a use of the notation

$$y \equiv u_\phi, \quad x \equiv \sqrt{\frac{2\alpha\omega}{V_{\rm A0}L}}z, \quad a \equiv -\frac{\omega}{V_{\rm A0}}\frac{L}{2\alpha} \quad (8)$$

Eq. (7) can be rewritten in the form of Weber (parabolic cylinder) equation (Abramowitz & Stegun 1964)

$$\frac{\partial^2 y}{\partial x^2} + \left(\frac{x^2}{4} - a\right)y = 0. \quad (9)$$

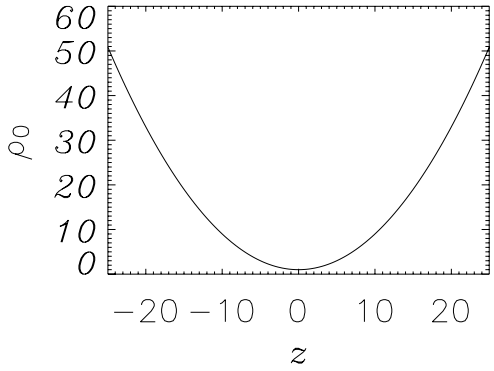


**Fig. 1.** Spatial profile of the background mass density, $\varrho_0(z)$, given by Eq. (6) with $\alpha^2 = 50$. The mass density and length are expressed in units of $10^{-12}$ kg m$^{-3}$ and 1 Mm, respectively.

Standard solutions to this equation are called Weber (parabolic cylinder) functions (Abramowitz & Stegun 1964)

$$W(a, \pm x) = \frac{(\cosh\pi a)^{1/4}}{2\sqrt{\pi}}\left(G_1 y_1(x) \mp \sqrt{2}G_3 y_2(x)\right), \quad (10)$$

where

$$G_1 = \left|\Gamma\left(\frac{1}{4} + \frac{{\rm i}a}{2}\right)\right|, \quad G_3 = \left|\Gamma\left(\frac{3}{4} + \frac{{\rm i}a}{2}\right)\right| \quad (11)$$

and $y_1(x)$, $y_2(x)$ are respectively even and odd solutions to Eq. (9)

$$y_1(x) = 1 + a\frac{x^2}{2!} + \left(a^2 - \frac{1}{2}\right)\frac{x^4}{4!} + \ldots,$$

$$y_2(x) = x + a\frac{x^3}{3!} + \left(a^2 - \frac{3}{2}\right)\frac{x^5}{5!} + \ldots$$

### 2.1. Two limiting solutions

Periodic solutions to Eq. (9) can be written analytically in the limiting cases: (a) for a large value of $a$ but a moderate value of $x$; (b) for a large $x$ but a moderate $a$. The first (second) case corresponds to $\alpha^2 \ll 1$ ($\alpha^2 \gg 1$).

#### 2.1.1. Weakly inhomogeneous plasma

We consider first the case of a weakly inhomogeneous mass density field, i.e. $\alpha^2 \ll 1$. In this case we have

$$a < 0, \quad -a \gg x^2, \quad p \equiv \sqrt{-a}. \quad (12)$$

We adopt the following expansion (Abramowitz & Stegun 1964):

$$W(a, x) + {\rm i}W(a, -x) = \sqrt{2}W(a, 0)\exp\left[v_{\rm r} + {\rm i}(px + \pi/4 + v_{\rm i})\right], \quad (13)$$

where

$$W(a, 0) = \frac{1}{2^{3/4}}\sqrt{\frac{G_1}{G_3}}, \quad (14)$$

$$v_{\rm r} = -\frac{(x/2)^2}{(2p)^2} + \frac{2(x/2)^4}{(2p)^4} + \ldots, \quad v_{\rm i} = \frac{2/3(x/2)^3}{2p} + \ldots \quad (15)$$

As a result of relation $-a \gg x^2$ we have from Eq. (13)

$$W(a,x) = \sqrt{2}W(a,0)\exp\left(-\frac{x^2}{16p^2}\right)\cos\zeta, \quad (16)$$

$$W(a,-x) = \sqrt{2}W(a,0)\exp\left(-\frac{x^2}{16p^2}\right)\sin\zeta, \quad (17)$$

$$\zeta \equiv px + \pi/4 + \frac{x^3}{24p}. \quad (18)$$

The general solution to Eq. (9) is

$$u_\phi = c_1 W(a,x) + c_2 W(a,-x), \quad (19)$$

where $c_1$ and $c_2$ are constants.

For a homogeneous loop, i.e. $\alpha^2 = 0$, we recognize the well known solution

$$u_\phi \sim c_1 \cos(kz + \pi/4) + c_2 \sin(kz + \pi/4). \quad (20)$$

Here wave number $k$ satisfies the following homogeneous dispersion relation:

$$k = \frac{\omega}{V_{A0}}. \quad (21)$$

Line-tying boundary conditions of Eq. (5) lead then to discrete values of the wave frequency, viz.

$$\omega_n = \frac{n\pi}{2L}\frac{V_{A0}}{1+\alpha^2/6}, \quad n = 1,2,3,\ldots \quad (22)$$

From this dispersion relation we infer that in a comparison to the loop with a homogeneous mass density distribution, $\varrho_{00}$, the weakly inhomogeneous mass density field results in a decrease of a wave frequency. This reduction is a consequence of the fact that the inhomogeneous loop is denser at its footpoints, so the average Alfvén speed is decreased. To show this, we compare the results for the inhomogeneous loop with the homogeneous loop of the same average density, so that both loops contain exactly the same mass (Andries et al. 2005). We introduce a frequency difference

$$\Delta\omega_n = \omega_n - \bar{\omega}_n, \quad (23)$$

where

$$\bar{\omega}_n = \frac{n\pi}{2L}\bar{V}_{A0} = \frac{n\pi}{2L}\frac{B_0}{\sqrt{4\pi\bar{\varrho}_0}} \quad (24)$$

corresponds to the average mass density

$$\bar{\varrho}_0 = \frac{1}{2L}\int_{-L}^{L}\varrho_0(z)\mathrm{d}z = \varrho_{00}\left(1+\frac{\alpha^2}{3}\right). \quad (25)$$

Substituting Eq. (25) into Eq. (24), we obtain

$$\bar{\omega}_n = \frac{n\pi}{2L}\frac{V_{A0}}{\sqrt{1+\alpha^2/3}}. \quad (26)$$

From Eqs. (23) and (26) we find that $\Delta\omega_n \leq 0$. Here we infer that in comparison to the average mass density case the wave frequency is reduced, but as a result of $\alpha^2 \ll 1$ the frequency reduction is small. This is in disagreement with Fermat's law and with the results of Murawski et al. (2004) who showed that sound waves experience frequency increase in a case of a space-dependent random mass density field.

#### 2.1.2. Strongly inhomogeneous plasma

We discuss now a strongly inhomogeneous mass density case, i.e. $\alpha^2 \gg 1$. This case corresponds to $x \gg |a|$. In this limit we get (Abramowitz & Stegun 1964)

$$W(a,x) = \sqrt{2k/x}(s_1(a,x)\cos(\xi) - s_2(a,x)\sin(\xi)), \quad (27)$$

$$W(a,-x) = \sqrt{2/kx}(s_1(a,x)\sin(\xi) - s_2(a,x)\cos(\xi)), \quad (28)$$

where

$$\xi \equiv \frac{x^2}{4} - a\ln x + \frac{\pi}{4} + \frac{\arg\Gamma(1/2+\mathrm{i}a)}{2}, \quad (29)$$

$$k = \sqrt{1+\mathrm{e}^{2\pi a}} - \mathrm{e}^{\pi a}, \quad (30)$$

$$s_1(a,x) \sim 1 + \frac{v_2}{1!2x^2} - \frac{u_4}{2!2^2x^4} - \cdots, \quad (31)$$

$$s_2(a,x) \sim -\frac{u_2}{1!2x^2} - \frac{v_4}{2!2^2x^4} + \ldots \quad (32)$$

with

$$u_r + \mathrm{i}v_r = \Gamma(r+1/2+\mathrm{i}a)/\Gamma(1/2+\mathrm{i}a), \quad r = 2,4,\ldots \quad (33)$$

The boundary conditions of Eq. (5) lead to the discrete frequency spectrum

$$\omega_n = \frac{n\pi}{\alpha}\frac{V_{A0}}{L}. \quad (34)$$

Here we infer that the strongly inhomogeneous mass density field results in a significant decrease of a wave frequency in comparison to the case of the loop with the constant density, $\varrho_{00}$. This wave frequency decrease is a consequence of the fact that the inhomogeneous loop is denser at its footpoints. Substituting Eq. (34) into Eq. (23) we find that $\Delta\omega_n > 0$. This wave frequency decrease, in comparison to the case of an average mass density is now in agreement with Fermat's law and with the results of Murawski et al. (2004).

## 3. Numerical results

Numerical simulations are performed for Eqs. (1), (2) with an adaptation of CLAWPACK which is a software package designed to compute numerical solutions to hyperbolic partial differential equations using a wave propagation approach (LeVeque 2002). The simulation region $(-L, L)$ is covered by a uniform grid of 600 numerical cells. We verified by convergence studies that this grid does not introduce much numerical diffusion and as a result it represents well the simulation region. We set reflecting boundary conditions at the left and right boundaries of the simulation region.

Figure 2 shows a spatial profile of velocity $u_\phi(z)$ for $\alpha^2 = 50$, drawn at $t = 1000$ s (solid line). This spatial profile results from the initial Gaussian pulse that was launched at $t = 0$ in the center of the simulation region, at $z = 0$. It is noteworthy that the sine-wave profile of Eq. (20), which is valid for $\alpha^2 = 0$ (dashed line), is distorted by the strong inhomogeneity which exists in the case of $\alpha^2 = 50$.

As a consequence of the inhomogeneity, the wave period is altered. Figure 3 displays wave period $P$ vs. inhomogeneity parameter $\alpha^2$. Diamonds represent the numerical solutions while the solid lines correspond to the analytical solution to Eqs. (22) (top panel) and (34) (bottom panel). Wave periods were obtained by a Fourier analysis of the wave signals that were collected in time at the fixed spatial location, $z = 0$. It is discernible that the numerical data fits quite well to the analytical curves. A growth

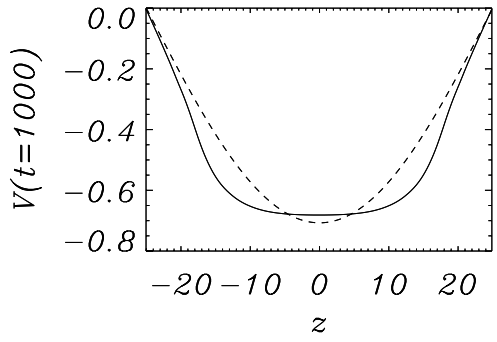


**Fig. 2.** Numerically evaluated velocity profile $u_\phi$ at $t = 1000$ s for $\alpha^2 = 50$ (solid line). This profile corresponds to the mode number $n = 1$. Note that as a result of strong inhomogeneity, $u_\phi$ departs from the sine-wave which corresponds to $\alpha^2 = 0$. The dashed line corresponds to Eq. (20) with $c_1 = c_2 = 0.5$.

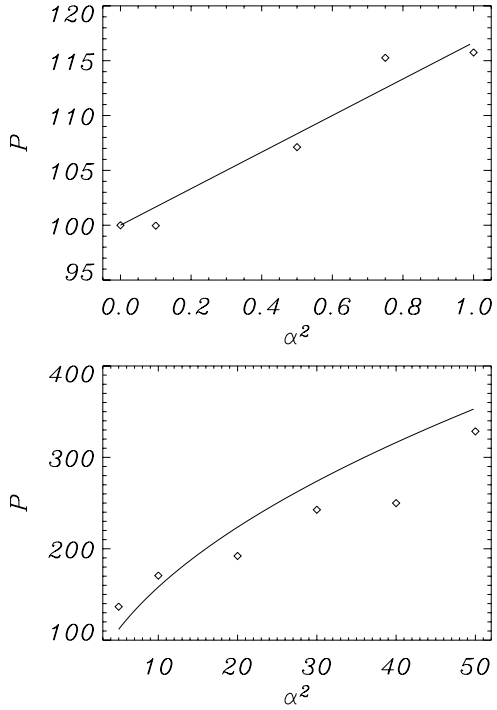


**Fig. 3.** Wave period $P = \omega/2\pi$ vs. $\alpha^2$ for the mode number $n = 1$. Diamonds correspond to the numerical solutions to Eqs. (1), (2). Solid lines are drawn with the use of the analytical solution to Eqs. (22) and (34). The wave period is expressed in seconds.

of wave period $P$ with $\alpha^2$ results from wave scattering on centers of the inhomogeneity and it can be explained on simple physical grounds. In an inhomogeneous field wave frequency $\omega_n$ of the torsional oscillations can be estimated from the following formula:

$$\omega_n = \frac{n\pi}{2L}\bar{V}_{A0}, \tag{35}$$

where $\bar{V}_{A0}$ is the averaged Alfvén speed that is expressed by Eq. (24). Using $P = 2\pi/\omega_n$ we obtain

$$P = \frac{4L\sqrt{4\pi\bar{\varrho}_0}}{nB_0}. \tag{36}$$

As $\bar{\varrho}_0$ grows with $\alpha$, the growth of $P$ with $\alpha$ results in.

## 4. Potential observations of torsional oscillations

Torsional oscillations of a coronal loop may result in periodic variations of spectral line non-thermal broadening (expressed by a half line width, $\Delta\lambda_B$, hereafter HW) (Zaqarashvili 2003). For a homogeneous loop, HW can be expressed as

$$\Delta\lambda_B = \frac{uV_{A0}\lambda}{c}|\sin(\omega_n t)\sin(k_n z)|, \tag{37}$$

where $u$ is an amplitude of oscillations, $\lambda$ is a wave length of the spectral line, and $c$ is the light speed. Periodic variations of spectral line width depend on the height above the solar surface: the strongest variation corresponds to the wave antinode and the place where there is a lack of line width variation corresponds to the nodes (loop footpoints). Therefore, a time series of spectroscopic observations may allow us to determine a wave period. Knowing a length of the loop, we may estimate the Alfvén speed, which in turn makes it possible to infer the magnetic field strength in the corona. We estimate the expected value of line width variations which result from torsional oscillations. For a typical coronal Alfvén speed of ~800 km s$^{-1}$, an amplitude of linear torsional oscillation can be ~40 km s$^{-1}$, which consists of 5% of the Alfvén speed. For the "green" coronal line Fe XIV (5303 Å) from Eq. (37) we obtain

$$\Delta\lambda_B \approx 0.7 \text{ Å}. \tag{38}$$

This value is about two times larger than the original thermal broadening of Fe XIV line. As a consequence, torsional oscillations can be detected in time series of the green coronal line spectra.

For a weakly inhomogeneous distribution of mass density along a loop, Eq. (22) enables us to estimate the Alfvén speed at the loop apex with the help of the observed period of HW variation and a loop length. For a strongly inhomogeneous density profile along a loop, Eq. (34) shows that a wave period of torsional oscillations is not just the ratio of the loop length to the Alfvén speed, but it strongly depends on the rate of inhomogeneity, $\alpha^2$. Therefore, an additional effort is required in order to apply the method of coronal seismology to torsional oscillations. A spatial variation of mass density along the loop can be estimated by a direct measurement of spectral line intensity variation along the loop. Then, the estimated variation can be fitted to Eq. (6), and hence a value of $\alpha^2$ can be inferred. Equation (34) provides a value of $V_{A0}$ at the loop summit. Another possibility is to collect time series of spectroscopic observations at different positions of the loop. A spatial variation of line width along the loop may be compared to the theoretical plot of $u_\phi$ (Fig. 2), which enables us to estimate $\alpha^2$ and consequently Alfvén speed at the loop apex (with a use of Eqs. (22) or (34)).

## 5. Discussion and summary

It is commonly believed that Alfvén waves are generated in the solar interior either by convection (granulation, supergranulation) or by other kinds of plasma flow (differential rotation, solar global oscillations). Due to their incompressible nature, these waves may carry energy from the solar surface to the solar corona and therefore they may significantly contribute to coronal heating and solar wind acceleration. In closed magnetic loops the Alfvén waves may set up the standing torsional oscillations, while in opened magnetic structures these waves may propagate up to the solar wind. As a result, observations of Alfvén waves can be of vital importance to the problems of plasma heating and particle acceleration.

The Alfvén waves that propagate along open magnetic field lines may lead to a growth of spectral line width with height (Hassler et al. 1990; Banerjee et al. 1998; Doyle et al. 1998). However, at some altitudes the spectral line width reveals a sudden fall off (Harrison et al. 2002; O'Shea et al. 2003, 2005). This phenomenon was recently explained by resonant energy transfer into acoustic waves (Zaqarashvili et al. 2006).

On the other hand, the photospheric motions may set up torsional oscillations in closed magnetic loop systems, which can be observed spectroscopically as periodic variations of spectral line width (Zaqarashvili 2003). As a result, the observation of Alfvén waves can be used as an additional powerful tool in coronal seismology; the observed period and loop mean length enables us to estimate the Alfvén speed within a loop, which in turn makes it possible to infer a mean magnetic field strength.

Besides their photospheric origin, Alfvén waves can be generated in the solar corona in a process of resonant absorption of the global oscillations (Ruderman & Roberts 2002; Goossens et al. 2002; Andries et al. 2005; Terradas et al. 2006). These oscillations may excite Alfvén waves in the outer inhomogeneous part of a loop, leading to attenuation of global oscillations and amplification of azimuthal oscillations. These Alfvén oscillations can be detected as periodic variations of spectral line width. As a consequence, observations of Alfvén waves can be a key for a determination of a damping mechanism of the loop global oscillations.

Dynamics of torsional Alfvén waves in a homogeneous loop can be solved easily. However, real coronal loops are longitudinally inhomogeneous, which leads to alteration of wave dynamics (Arregui et al. 2005, 2007; Van Doorsselaere et al. 2004a,b; Donnelly et al. 2006; Dymova & Ruderman 2006; McEwan et al. 2006). Therefore, the dynamics of Alfvén waves in longitudinally inhomogeneous coronal loops must be understood in order to provide an analytical basis for potential observations of torsional oscillations.

In this paper we discussed the evolution of torsional Alfvén waves in inhomogeneous mass density fields using analytical and numerical methods. The analytical efforts resulted in dispersion relations which were obtained for a specific choice of equilibrium mass density profile. These dispersion relations were written explicitly for two limiting cases: (a) weekly inhomogeneous and (b) strongly inhomogeneous mass density fields. From these dispersion relations we inferred that the inhomogeneity results in a wave frequency reduction in comparison to that estimated at the loop summit. This analytical finding is supported by the numerical data which reveals that frequency reduction takes place outside the region of validity of the analytical approach. As a result of that we claim that a reduction of wave frequency is ubiquitous for the inhomogeneous mass density field we considered. This reduction is a consequence of wave scattering on inhomogeneity centers and it results from reduction of the average Alfvén speed within a coronal loop. This frequency reduction has important implications as far as wave observations are concerned. The analytical formulae can be used for estimation of coronal plasma parameters and therefore torsional Alfvén waves are a powerful tool of coronal seismology.

*Acknowledgements.* The authors express their thanks to the referee, Prof. S. Poedts, for his stimulating comments. The work of T.Z. is supported by the grant of Georgian National Science Foundation GNSF/ST06/4-098. A part of this paper is supported by the ISSI International Programme "Waves in the Solar Corona".

## References

Abramowitz, M., & Stegun, I. A. 1964, Handbook of Mathematical Functions (Washington, D.C.: National Bureau of Standards)
Andries, J., Goossens, M., Hollweg, J. V., Arregui, I., & Van Doorsselaere, T. 2005, A&A, 430, 1109
Arregui, I., Van Doorsselaere, T., Andries, J., Goossens, M., & Kimpe, D. 2005, A&A, 441, 361
Arregui, I., Andries, J., Van Doorsselaere, T., Goossens, M., & Poedts, S. 2007, A&A, 463, 333
Aschwanden, M. J., Fletcher, L., Schrijver, C. J., & Alexander, D. 1999, ApJ, 520, 880
Banerjee, D., Teriaca, L., Doyle, J., & Wilhelm, K. 1998, A&A, 339, 208
De Moortel, I., Ireland, J., Walsh, R. W., & Hood, A. W. 2002, Sol. Phys., 209, 61
Diáz, A., Zaqarashvili, T. V., & Roberts, B. 2006, A&A, 455, 709
Donnelly, G. R., Diáz, A., & Roberts, B. 2006, A&A, 457, 707
Doyle, J., Banerjee, D., & Perez, M. 1998, Sol. Phys., 181, 91
Dymova, M. V., & Ruderman, M. S. 2006, A&A, 457, 1059
Edwin, P. M., & Roberts, B. 1982, Sol. Phys., 76, 239
Edwin, P. M., & Roberts, B. 1983, Sol. Phys., 88, 179
Goossens, M., Andries, J., & Aschwanden, M. J. 2002, A&A, 394, L39
Gruszecki, M., Murawski, K., Solanki, S., & Ofman, L. 2007, A&A (in press)
Harrison, R. A., Hood, A. W., & Pike, C. D. 2002, A&A, 392, 319
Hassler, D. M., Rottman, G. J., Shoub, E. C., & Holzer, T. E. 1990, ApJ, 348, L77
LeVeque, R. J. 2002, Finite Volume Methods for Hyperbolic Problems (Cambridge University Press)
McEwan, M. P., Donnelly, G. R., Diaz, A. J., & Roberts, B. 2006, A&A, 460, 893
Murawski, K., Nocera, L., & Pelinovsky, E. N. 2004, Waves in Random Media, 14, 109
Nakariakov, V. M. 2003, in The Dynamic Sun, ed. B. Dwivedi (CUP)
Nakariakov, V. M., & Ofman, L. 2001, A&A, 372, L53
Nakariakov, V. M., Ofman, L., Deluca, E. E., Roberts, B., & Davila, J. M. 1999, Science, 285, 862
O'Shea, E., Banerjee, D., & Poedts, S. 2003, A&A, 400, 1065
O'Shea, E., Banerjee, D., & Doyle, J. G. 2005, A&A, 436, L35
Ofman, L. 2005, Adv. Space Res., 36, 1772
Pascoe, D. J., Nakariakov, V. M., & Arber, T. D. 2007, A&A, 461, 1149
Poedts, S., & Boynton, G. C. 1996, A&A, 306, 610
Roberts, B. 2000, Sol. Phys., 193, 139
Ruderman, M. S., & Roberts, B. 2002, ApJ, 577, 475
Terradas, J., Oliver, R., & Ballester, J. L. 2006, ApJ, 642, 533
Verwichte, E., Foullon, C., & Nakariakov, V. M. 2006, A&A, 449, 769
Wang, T., Solanki, S. K., Innes, D. E., Curdt, W., & Marsch, E. 2003, A&A, 402, L17
Wang, T. J., & Solanki S. K. 2004, A&A, 421, L33
Zaqarashvili, T. V. 2003, A&A, 399, L15
Zaqarashvili, T. V., Oliver, R., & Ballester, J. L. 2006, A&A, 456, L13
Van Doorsselaere, T., Andries, J., Poedts, S., & Goossens, M. 2004a, ApJ, 606, 1223
Van Doorsselaere, T., Debosscher, A., Andries, J., & Poedts, S. 2004b, A&A, 424, 1065